ANALYSING THE CAPABILITY OF SENTINEL-1 SAR DATA FOR FLOOD MONITORING AND MAPPING IN IDUKKI DAM RESERVOIR, SOUTHERN WESTERN GHATS OF INDIA

Sumith S. S. and John C. M.

Dr. R. Satheesh Centre for Remote Sensing & GIS, School of Environmental Sciences,
Mahatma Gandhi University, Kottayam, Kerala, India - 686560
Email: rsgismgu@gmail.com

KEY WORDS: Microwave, Submergence, Synthetic Aperture Radar, Multi-temporal

ABSTRACT: Efficient monitoring and prediction of floods and risk management for large reservoir is impossible without the use of Earth Observation data from space. One of the most important problems associated with flood monitoring is the difficulty to determine the extent of the flood area as even a dense network of observations cannot provide such information. The flood extent information is used for damage assessment and risk management. The use of optical imagery for flood monitoring is limited by the presence of clouds. In turn, Synthetic Aperture Radar (SAR) measurements from space are independent of daytime and weather conditions and can provide valuable information to monitor flood events. This is mainly due to the fact that smooth water surface provides no return to antenna in microwave spectrum and appears black in SAR imagery.
This study explored large inundation areas in the Idukki Reservoir in Kerala state. Sentinel-1A image with C-band and dual-polarization capability (HH+HV or VV+VH) was used in the study. This study aims to analyses Sentinel-1 SAR data for its potential to map standing water in the Idukki reservoir.15 SAR images of Level-1 Ground Range Detected (GRD) C-band (5.405 GHz) collected in the Interferometric Wide Swath (IW) mode -during the period from January 2016 to December 2016 - were used to develop a procedure for reliable processing. These time-series SAR images were utilized to investigate the multi-temporal variation of different water extent across the Idukki reservoir area and to classify the water from land area. Field verification carried out on 26th May, 2016, 6th June 2016 and 2nd December 2016 to find the current standing water in the reservoir. The permanent water body extent line vectorised from Google earth image dated 2nd March 2013 on which the lowest flood extent was recorded for the last ten years.

1. INTRODUCTION

Remote sensing data has been widely used for flood mapping and monitoring. If optical data's utility in flood detection depends on cloud cover, active remote sensing with all-weather monitoring capability and its large coverage is an important tool in flood monitoring (Trinh Le Hung, 2007), Flood monitoring and mapping using Earth Observation (EO) data can help authorities and non-governmental organizations in disaster management and coordination of humanitarian efforts. Data from both optical and microwave sensors can be used for flood mapping. The present study aims to analyze Sentinel-1 SAR data for its potential to map flood extent over the Idukki Dam Reservoir, around the eastern part of Kerala state, as determined from passive sensor data and the cloud-penetrating capabilities of the active sensors of the remote imaging microwave Sentinel-1.

Idukki Dam is the World's First Arch dam. It is 554 feet tall, constructed between the two mountains - Kuravanmala (839 meters) and Kurathimala (925 meters). This project is situated in Idukki District and its underground power house is located at Moolamattom which is about 43 km from the dam. Twice in the past, the shutters (of Cheruthoni) had to be opened; during the northeast monsoon (October to December) on both occasions. The first time was in 1981 (when the shutters were repeatedly opened and shut between October 29 and November 13) and the second time was in 1992 (when they were kept open for 12 days from October 12 to 23). On both occasions, the water level in the dam touched the brim only when the storage built up during the southwest monsoon (June to September) was augmented by the inflow received immediately afterwards following heavy downpour early in the northeast monsoon.

1.1 Usage Importance of the Dam

1.1.1 Power Generation: The Project harnesses a major portion of the power potential of Periyar, the largest river in Kerala, by the creation of a reservoir of 2,000 M.cum (2 Billion Tonnes) capacity, diversion of waters thus impounded through a water conductor system consisting of a power tunnel and two underground pressure shafts to an underground power house situated in Moolamattom. It was constructed and is owned by the Kerala State Electricity Board (KSEB). It supports a 780 MW hydroelectric power station in Moolamattom, which started generating power on 4 October 1975 technically; the dam type is a concrete double, curvature parabolic, thin arch dam. The installed capacity of the Power House is 780MW consisting of 6 Units of Pelton-type turbines with a power generation capacity of 130 MW each. The regulated waters of Periyar falls through a drop of about 669.2 metres (2195 feet) while generating power in the underground power house.

1.1.2 Irrigation: The tail waters flowing to Kudayathurpuzha through tunnel and open channel is diverted for irrigation purposes in the Muvattupuzha Valley.

1.1.3 Tourist destination and attraction: Earlier, there was a blanket ban on public entry in to the dam due to security reasons. Later, it was relaxed opening the dam for public for 10 days during the Onam and the Christmas seasons. The duration has been increased to one month since last year. Cameras and cell phones are not allowed inside the dam area. Idukki valley is 121 km away from Kottayam, and is a small hill town surrounded by a spread of beautiful, wooden valleys and meandering streams. Idukki is a well-known tourist center in Kerala. The Idukki Wildlife Sanctuary extends over the Thodupuzha and Udumbanchola taluks of Idukki district, spread over 77 km^2 and is about 450 – 748 m above sea level. The Idukki Reservoir formed by three dams - Cheruthoni, Idukki and Kulamavu - extends to 33 km^2. One can find Elephants, bisons, sambars deers, wild dogs, jungle cats, tigers, wild boars etc. and variety of Snakes like Cobra, viper, krait and a number of non-poisonous snakes in this Sanctuary. The birds of Idukki are Jungle fowl, myna, laughing thrush, black bulbul, peafowl, woodpecker, kingfisher etc.

1.2 The present study

To delineate the flood extent of Idukki dam reservoir and mapping water extent using Multi-temporal Sentinel-1 Microwave Satellite datasets of Pre, During and Post Monsoon of the year 2016.

2. STUDY AREA

The Idukki Dam is a double curvature arch dam constructed across the Periyar River in a narrow gorge between two granite hills Kuravan and Kurathi in Kerala, India. At 167.68 metres, it is one of the highest arch dams in Asia. This dam was constructed along with two other dams at Cheruthoni and Kulamavu. Together, the three dams have created an artificial lake that is 60 km^2 in area (Fig. 1 and 2). The stored water is used to produce electricity at the Moolamattom Power house, which is located inside nearby rocky caves. The Government of Canada aided in the building of the dam with long term loans and grants.

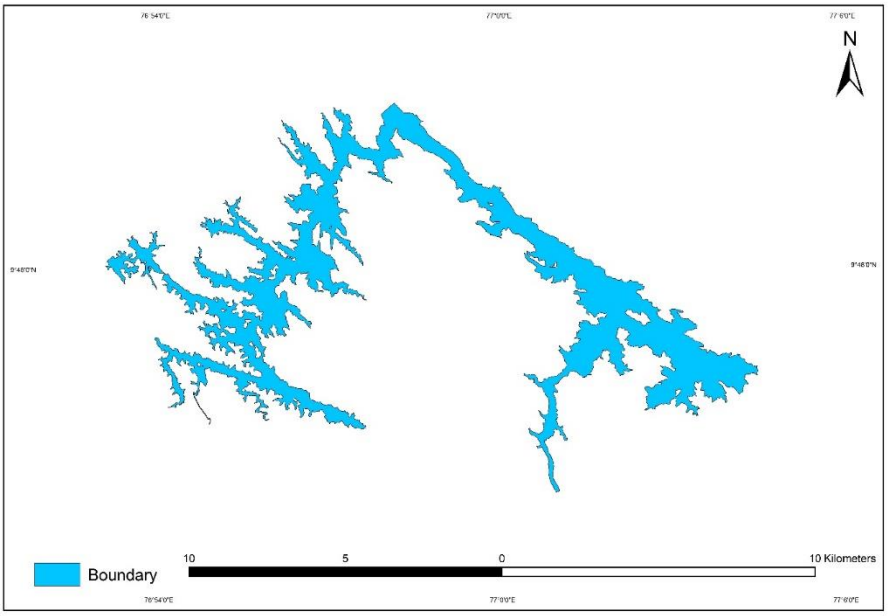

Figure 1: Water level extent of the Reservoir on 2nd March 2013

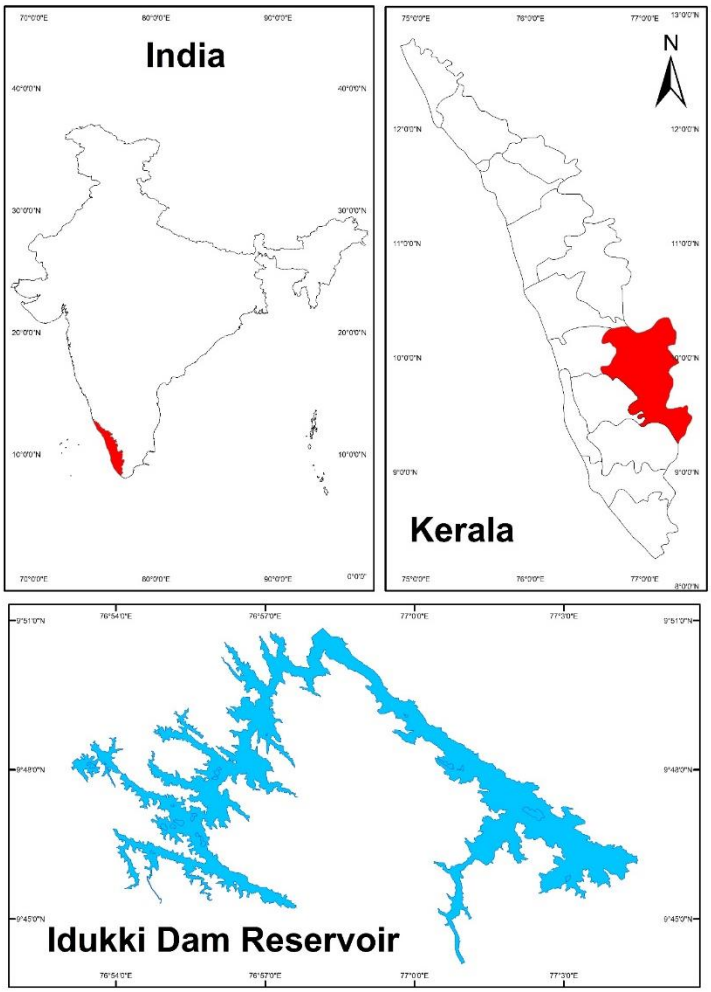

Figure 2: Study area – Location: Idukki Dam Reservoir

Figure 3: Field Photographs (2nd March 2013)

3. MATERIALS AND METHODS

3.1 Data and Software Used

3.1.1 Sentinel-1 data: In this study, Level-1 Ground Range Detected (GRD) Sentinel-1 C-band (5.405 GHz) data collected in the Interferometric Wide swath (IW) mode were used. This mode allows the combination of a large swath width (250 km) with a moderate geometric resolution (10m). Images are freely available from the European Space Agency (ESA) through Sentinels Scientific Data Hub (SSDH 2017) (https://scihub.esa.int/dhus/). The time interval of the acquired images varies from 11 days up to 30 days. The main characteristics of the collected Sentinel -1 IW data are provided in Table 1. The IW mode is the default acquisition mode over land. The user guide (https://sentinel.esa.int/web/sentinel/user-guides/sentinel-1-sar) provides further information on the satellite's acquisition parameters (Table 2) (Fig. 8).

The above data were used to develop a procedure for reliable processing of the Sentinel-1 SAR images. Fifteen SAR images have been collected during the period from 4th January 2016 to 5th December 2016. Sentinel-1 images with spatial resolution of 10 m by 10 m were used for frequency analysis of water extent from January to December 2016. SENTINEL-1 remote sensing data, Water Level data, and ground data were used for the purpose of flood monitoring, mapping and assessing. A threshold based classification was used for this demarcation of land and water. They were processed for creating a maximum water extent map and for estimating inundation areas.

Table 1: Sentinel-1 data acquisition modes and resolution

Mode	Access Angle	Single Look Resolution	Swath Width	Polarization
Interferometric Wide Swath	> 25 deg.	Range 5m Azimuth 20 m	> 250 km	HH+HV or VV+VH
Wave mode	23 deg. and 36.5 deg.	Range 5m Azimuth 5 m	> 20x20 km Vignettes at 100 km intervals	HH or VV
Strip Map	20 - 45 deg.	Range 5m Azimuth 5 m	> 80 km	HH+HV or VV+VH
Extra Wide Swath	> 20 deg.	Range 20 m Azimuth 40 m	> 250 km	HH+HV or VV+VH

Table 2: Characteristics of the Sentinel-1 Interferometric Wide swath mode nominal measurement modes

Parameter	Interferometric Wide-swath mode (IW)
Swath width	250 km
Incidence angle range	29.1° - 46.0°
Sub-swaths	3
Azimuth steering angle	± 0.6°
Azimuth and range looks	Single
Polarization options	Dual VV+VH
Maximum Noise Equivalent Sigma Zero (NESZ)	-22 dB
Radiometric stability	0.5 dB (3σ)
Pixel size (meter)	10

The polarization of SAR images refers to the geometric plane that the radar wavelength is transmitted and received along. In most systems these are either horizontal (H) or vertical (V) in relation to the satellite antenna, creating four common polarizations: HH, HV, VH, and VV. Although each polarization can be used for flood delineation, the backscatter characteristics of the radar signal varies, impacting the accuracy of the inundation maps produced. (Manjusree et al., 2012), compared the four polarizations, concluding that HH has the greatest potential for delineating flooding consistently and accurately, results mirrored in other research (Henry et al., 2006; Brisco et al., 2008), Sentinel-1 collects images in VH and VV polarization when in IW mode, both of which have the potential for classification errors. Cross-polarized data (VH and HV) produces a wider range of backscatter values from vegetated land surfaces compared to co-polarized data (VV and HH), leading to potential overlap with the low backscatter values associated with water, causing misclassification of land as flooded (Manjusree et al., 2012; Twele et al., 2016), VV polarized wavelengths are more susceptible to roughening of the water surface, commonly caused by wind or rain, increasing the backscatter return to the satellite, resulting in inundation not being identified (Manjusree et al., 2012), The limitations of each polarization as environmental conditions vary requires acknowledgement when using Sentinel-1 for flood mapping. Previous research concluded that under calm wind conditions VV provides a slightly higher thematic accuracy than VH polarized data for identifying flooding when using Sentinel-1 data (Twele et al., 2016),

3.1.2 Software used:

- Sentinel Application Platform (SNAP 5.0)
- Quantum-GIS (Q-GIS 2.18)

3.2 Methods

3.2.1 Sentinel-1 Data Pre-Processing: SNAP software (Sentinels Application Platform) particularly the S-1 Tool box of the SNAP was utilized to pre-process the SAR imagery. SAR data can be accessed by targeting the entire Sentinel ZIP file in SNAP. The original SAR image is inverted in the SNAP. It is displayed according to the order of data acquisition, which is not according to a cartographic representation. Furthermore, the synthetic method used for creating the SAR imagery also has some disadvantages. Inherent to the measurement technique is random constructive and destructive interference of waves which cause the SAR images to be noisy. This noise within the SAR images is called speckle and decreases the quality of the image and making interpretation of features more difficult. A number of speckle filter types are provided in SNAP. Speckle noise reduction was applied by using single product speckle filter (Fig. 4).

Speckle filtering is needed to suppress the noise in order to allow better interpretation and backscatter analysis. However, speckle filters not only suppress the noise, but also remove observations that are not affected by noise and contain valuable land surface information (e.g. soil moisture, biomass and flood extent). Here, single product speckle filter method in SNAP was used to remove the speckle. The SNAP S-1 Tool box operator supports the following speckle filter types for handling speckle noise of different distributions (Gaussian, multiplicative or Gamma): Mean, Median, Lee, Refined Lee, and Gamma-MA. Lee Filter is based on multiplicative speckle model and uses local statistics to preserve details. Lee filter works on the variance basis, i.e. If variance of the area is low then it performs smoothing operation but not for high variance. That means it can preserve details in low as well as in high contrast hence it has adaptive nature (Jyoti Jaybhay and Rajveer Shastri, 2015), hence the present study used Lee sigma filter with 7x7 window size.

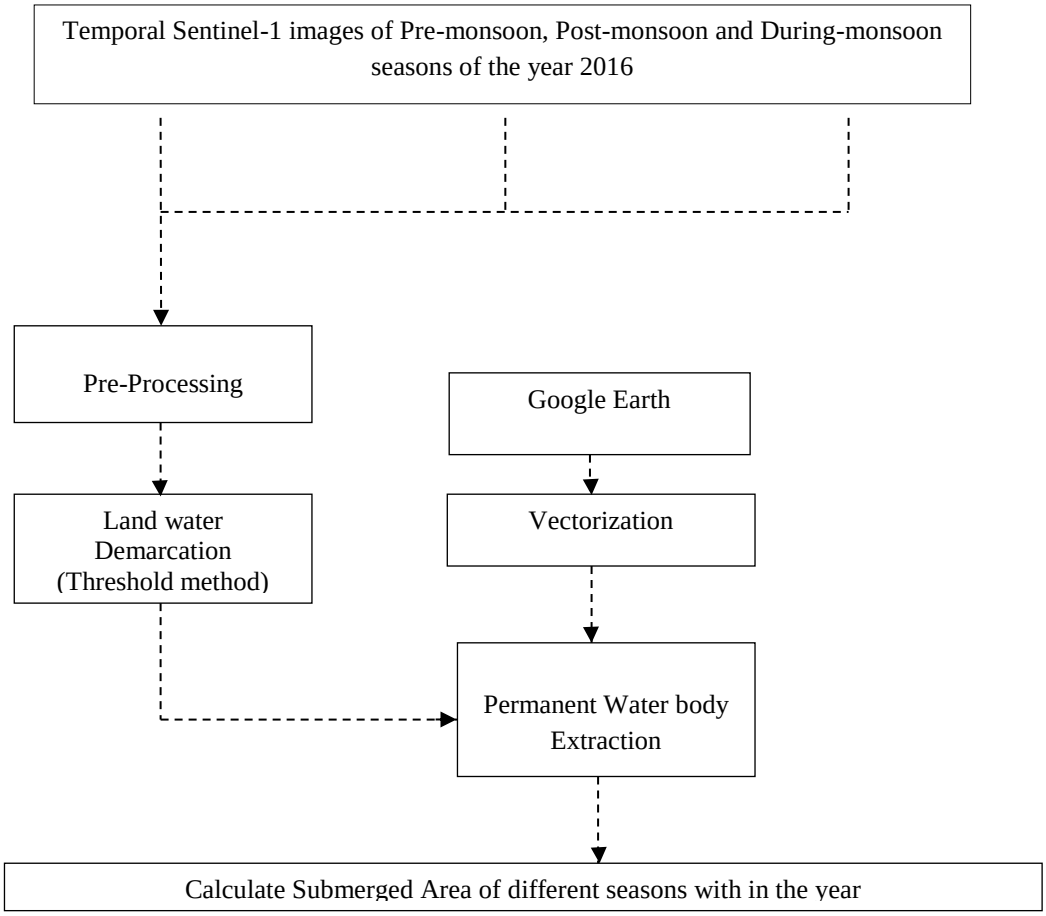

Figure 4: Steps adopted for Sentinel-1 data processing

To re-project the images from geometry of the sensor to the geographic projection, terrain correction was applied. The Processing Parameters are, Digital Elevation Model (SRTM-3Sec) (Auto Download) DEM over the region that SAR image covers will be automatically downloaded; DEM Resampling Method – Bilinear Interpolation; Image Resampling Method – Nearest Neighbor; Pixel Spacing - 10 m (which is depending on the sensor and its acquisition mode); Map projection - WGS84.

Thresholding method is used for delineating water from non-water. For this an average threshold value of 5 SAR images 1.93 E^{-2}, 2.52 E^{-2} and 2.25 E^{-2} for pre, during, and post monsoon respectively is used to separate water. The Symmetrical Difference tool was used to find the area in which the inundated area reference with the permanent water body extent line vectorised from Google earth image dated 2nd March 2013 on which the lowest flood extent was recorded for the last ten years. The each dataset of pre, during and post monsoon data was symmetrically difference with permanent water body extent. From these overlaying analysis the flooded Area of the reservoir in different seasons with in the year were calculated.

4. RESULTS AND DISCUSSION

In the analysis dual polarized SAR images from different date were used to detect the flood extent. A one year period around fifteen datasets have been analysed as pre, during and post monsoon respectively. Between 12th September and 18th October was the peak inundated period in the year 2016 (Fig. 5 to 7). By analyzing Tables 3 and 4, it is clear that more area submerged on 31st and 14th July. The near date water level data of reservoir were also very high from 23rd August onwards (India WRIS, 2017).

Table 3: Extent of submerged areas in different seasons of 2016

Pre Monsoon	Area (ha)	During Monsoon	Area (ha)	Post Monsoon	Area (ha)
04-Jan-16	280.33	08-Jun-16	61.00	6-0ct-2016	307.28
09-Feb-16	291.63	02-Jul-16	99.95	18-Oct-16	291.99
04-Mar-16	190.04	31-Aug-16	273.36	30-Oct-16	260.64
15-May-16	29.04	12-Sep-16	327.39	11-Nov-16	248.61
27-May-16	28.49	24-Sep-16	177.99	05-Dec-16	273.30

Table 4: Water Level Data of the reservoir in different seasons of 2016

Pre Monsoon	Level (m)	During Monsoon	Level (m)	Post Monsoon	Level (m)
04-Jan-16	720.580	08-Jun-16	705.411	05-Oct-16	716.420
09-Feb-16	718.139	20-Jul-16	713.013	13-Oct-16	716.073
04-Mar-16	715.817	23-Aug-16	716.359	20-Oct-16	716.010
15-May-16	707.075	08-Sep-16	716.850	26-Oct-16	715.670
27-May-16	705.917	20-Sep-16	716.730	10-Nov-16	715.384

(Source: India WRIS, 2017)

Table 5: Percentage of submerged areas in different seasons of 2016

Pre Monsoon	Area (%)	During Monsoon	Area (%)	Post Monsoon	Area (%)
04-Jan-16	34.21	08-Jun-16	6.49	6-0ct-2016	22.24
09-Feb-16	35.58	02-Jul-16	10.64	18-Oct-16	21.13
04-Mar-16	23.19	31-Aug-16	29.09	30-Oct-16	18.86
15-May-16	3.54	12-Sep-16	34.84	11-Nov-16	17.99
27-May-16	3.48	24-Sep-16	18.94	05-Dec-16	19.78

Submergence was more in the post monsoon season in the reservoir area. It is found that the peak flood event occurred on 12th September. By analyzing Table 4 and nearby date water level data, it is clear that more area submerged on 1st September to 20th October. In the pre monsoon season on 4th January 280.33ha area of land area were submerged. Which means 34.21 % of land was inundated. On 9th February, 4th March, 15th May and 27th May the inundated area were 291.63ha, 190.04ha, 29.04ha, 28.49ha and the percentage were 35.58%, 23.19%, 3.54% and 3.48% respectively. The during monsoon season to post monsoon the extent of the water was increased gradually. That was on 8th June 61ha land area were submerged that was around of 6.49% of the total percentage. On 2nd July, 31st August, 12th September and 24th September the inundated area were 99.95ha, 273.36ha, 327.39ha, 177.99ha and the percentage were 10.64%, 29.09%, 34.84% and 18.94% respectively. The beginning of post monsoon on 6th October around 307.28ha land area were submerged by the flooded water. Which was around the 22.24% of the total percentage. On 18th October, 30th October, 11th November and 5th December the inundated area were 291.99ha, 260.64ha, 248.61ha,

273.30ha and the percentage were 21.13%, 18.86%, 17.99% and 19.78% respectively (Table 5). As a result of continuous raining on 23rd August to 20th October, the submergence extent drastically increased and the tributaries of Idukki dam reservoir contribute high volume of water to the reservoir.

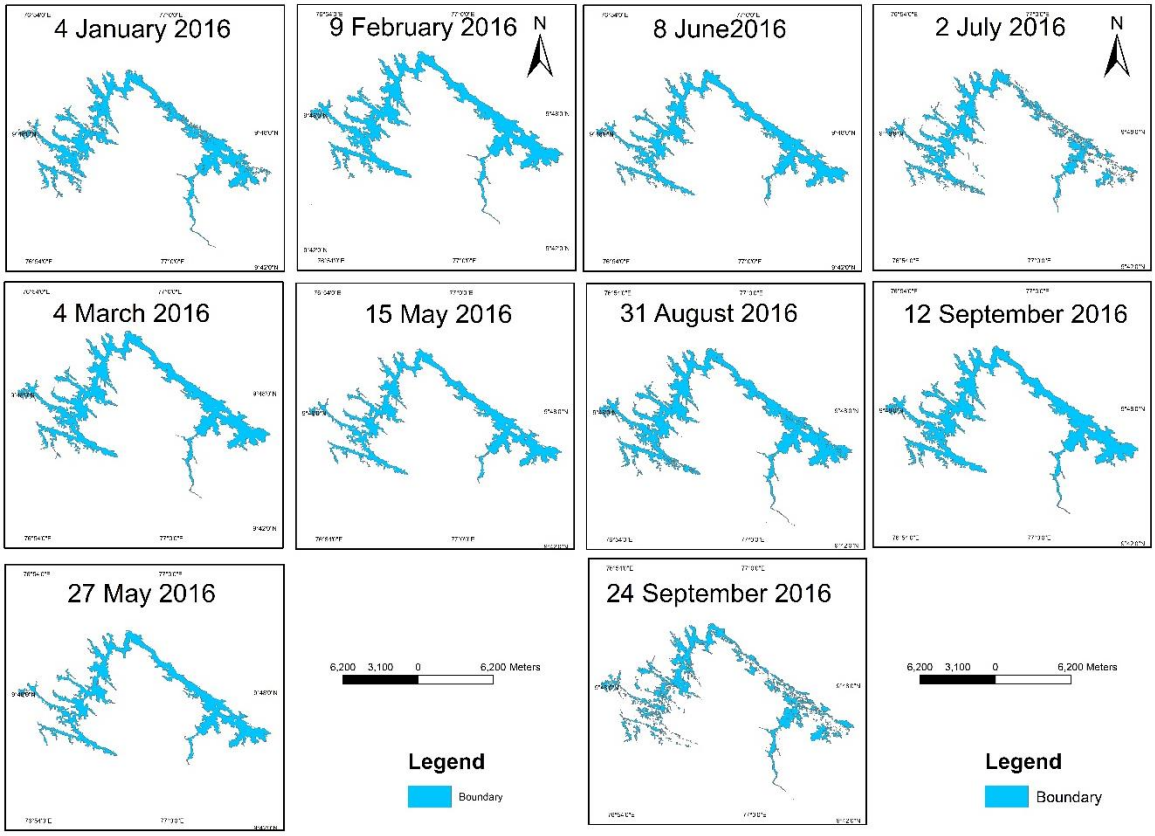

Figure 5: Water extent of pre monsoon season

Figure 6: Water extent of during monsoon season

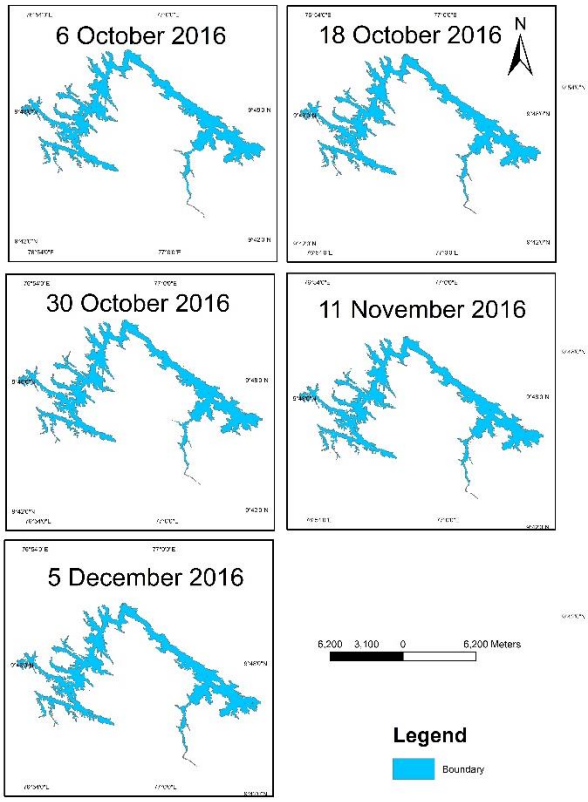

Figure 7: Water extent of post monsoon season

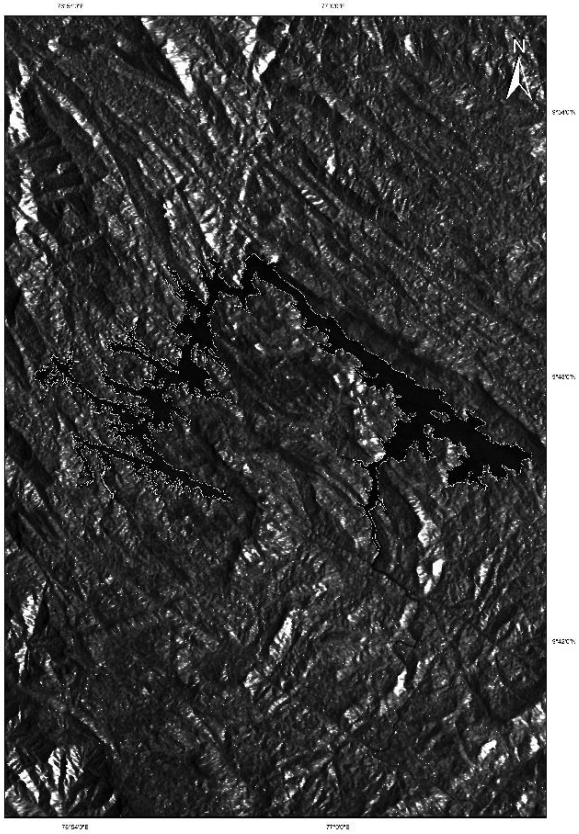

Figure 8: Sentinel-1 imagery of the study area

5. CONCLUSION

The Flood monitoring using SAR data proved to be an effective method to get quick and precise overview of flooded areas. In this study, timely and detailed analysis had been carried out using Remote Sensing & GIS tools for locating and identifying flooded areas under various seasons in the year of 2016. Due to the cloud cover and rain it is very difficult to use an optical satellite imagery. It was found that this method requires processed satellite images which is very useful for water inundated area estimation. The methodology used in this study has the capability to carryout land water demarcation.

REFERENCES

Brisco B., Touzi R., van der Sanden J.J., Charbonneau F., Pultz T.J. & and D'lorio M., 2008. Water resourceWater resource applications with RADARSAT-2 – a preview. International Journal of Digital Earth 2008, 1, (1), pp.130–147.

Henry J. B., Chastanet P., Fellah K. & and Desnos Y. L., 2006. Envisat multipolarized ASAR data for flood mapping. International Journal of Remote Sensing 2006, 27, (9–10), pp.1921–1929.

India WRIS., 2017. India Water Resource Information System. Retrieved JanuaryRetrieved January 4, 2017, from http://india-wris.nrsc.gov.in/ReservoirApp.html?UType=R2VuZXJhbA==?UName=.

Jyoti Jaybhay and Rajveer Shastri, 2015 June. "A study of speckle noise reduction Filters". International Journal of Signal & and Image Processing,: Anan International Journal (SIPIJ))Vol.6, 6, No.3, June 2015.(3), pp. 71-80..

Manjusree R., Kumar L.P., Bhatt C.M., Rao G.S. & and Bhanumurthy V., 2012.Optimization of threshold ranges for rapid flood inundation mapping by evaluating backscatter profiles of high incidence angle SAR images. International Journal of Disaster Risk Science 2012, 3, (2), pp.113–122.

Trinh Le Hung,. 2007. Retrieved January 4, 2017, from http://old.pskgu.ru/projects/pgu/storage/we6137/wepgu03/wepgu_03_06.pdf.

Twele A., Cao W.X., Plank S. & and Martinis S., 2016. Sentinel-1-based flood mapping: a fully automated processing chain. International Journal of Remote Sensing 2016, 37, (13), pp. 2990–3004.